

Neuron-Specific Deletion of Peroxisome Proliferator-Activated Receptor Delta (PPAR δ) in Mice Leads to Increased Susceptibility to Diet-Induced Obesity

Heidi E. Kocalis¹, Maxine K. Turney³, Richard L. Printz¹, Gloria N. Laryea⁴, Louis J. Muglia^{1,6}, Sean S. Davies⁵, Gregg D. Stanwood⁵, Owen P. McGuinness¹, Kevin D. Niswender^{2,1,3*}

1 Department of Molecular Physiology and Biophysics, Vanderbilt University School of Medicine, Nashville, Tennessee, United States of America, **2** Department of Veterans Affairs, Tennessee Valley Healthcare System, Nashville, Tennessee, United States of America, **3** Department of Medicine, Division of Diabetes, Endocrinology and Metabolism, Vanderbilt University School of Medicine, Nashville, Tennessee, United States of America, **4** Neuroscience Graduate Program, Vanderbilt University, Nashville, Tennessee, United States of America, **5** Department of Pharmacology, Vanderbilt University School of Medicine, Nashville, Tennessee, United States of America, **6** Department of Pediatrics, Vanderbilt University School of Medicine, Nashville, Tennessee, United States of America

Abstract

Central nervous system (CNS) lipid accumulation, inflammation and resistance to adipo-regulatory hormones, such as insulin and leptin, are implicated in the pathogenesis of diet-induced obesity (DIO). Peroxisome proliferator-activated receptors (PPAR α , δ , γ) are nuclear transcription factors that act as environmental fatty acid sensors and regulate genes involved in lipid metabolism and inflammation in response to dietary and endogenous fatty acid ligands. All three PPAR isoforms are expressed in the CNS at different levels. Recent evidence suggests that activation of CNS PPAR α and/or PPAR γ may contribute to weight gain and obesity. PPAR δ is the most abundant isoform in the CNS and is enriched in the hypothalamus, a region of the brain involved in energy homeostasis regulation. Because in peripheral tissues, expression of PPAR δ increases lipid oxidative genes and opposes inflammation, we hypothesized that CNS PPAR δ protects against the development of DIO. Indeed, genetic neuronal deletion using Nes-Cre loxP technology led to elevated fat mass and decreased lean mass on low-fat diet (LFD), accompanied by leptin resistance and hypothalamic inflammation. Impaired regulation of neuropeptide expression, as well as uncoupling protein 2, and abnormal responses to a metabolic challenge, such as fasting, also occur in the absence of neuronal PPAR δ . Consistent with our hypothesis, KO mice gain significantly more fat mass on a high-fat diet (HFD), yet are surprisingly resistant to diet-induced elevations in CNS inflammation and lipid accumulation. We detected evidence of upregulation of PPAR γ and target genes of both PPAR α and PPAR γ , as well as genes of fatty acid oxidation. Thus, our data reveal a previously underappreciated role for neuronal PPAR δ in the regulation of body composition, feeding responses, and in the regulation of hypothalamic gene expression.

Citation: Kocalis HE, Turney MK, Printz RL, Laryea GN, Muglia LJ, et al. (2012) Neuron-Specific Deletion of Peroxisome Proliferator-Activated Receptor Delta (PPAR δ) in Mice Leads to Increased Susceptibility to Diet-Induced Obesity. *PLoS ONE* 7(8): e42981. doi:10.1371/journal.pone.0042981

Editor: Antonio Moschetta, University of Bari & Consorzio Mario Negri Sud, Italy

Received: February 16, 2012; **Accepted:** July 16, 2012; **Published:** August 20, 2012

This is an open-access article, free of all copyright, and may be freely reproduced, distributed, transmitted, modified, built upon, or otherwise used by anyone for any lawful purpose. The work is made available under the Creative Commons CC0 public domain dedication.

Funding: The project is supported by National Institutes of Health grants DK085712, DK069927, DK007563 (KDN) and DK083222 (to HK) and partially by DK058404 (KDN), the Vanderbilt Diabetes Research and Training Center (DRTC) (DK20593 to KDN) and the DRTC Mouse Metabolic Phenotyping Center (MMPC DK59637 to KDN). This work was partially supported by resources of the Vanderbilt University Translation Pathology Shared Resource Core (5U24 DK059637). The funders had no role in study design, data collection and analysis, decision to publish, or preparation of the manuscript.

Competing Interests: The authors have declared that no competing interests exist.

* E-mail: kevin.niswender@vanderbilt.edu

Introduction

Obesity is a serious health problem in the United States and worldwide [1,2]. Evidence indicates that body weight and adiposity can be tightly physiologically regulated through the coordinated action of distributed neurons and brain circuits, which regulate feeding and energy expenditure in response to changes in circulating hormones [3] and nutrients [4]. Dietary fat consumption, in particular, is associated with weight gain, obesity and metabolic disease [5,6,7,8]. Consumption of a high-fat diet (HFD) has been shown to lead to lipid accumulation and inflammatory signaling in key neuronal subsets involved in the regulation of energy homeostasis [9,10,11,12], resulting in behavioral and biochemical resistance to insulin, leptin and other regulatory hormones and nutrient signals in the CNS.

In order to understand the effects of dietary fat on obesity predisposition, we sought to identify molecular metabolic regulators that may be lipid sensitive. Peroxisome proliferator-activated receptor δ (PPAR δ) is a member of the PPAR family of nuclear receptors, a class of lipid activated transcription factors belonging to the nuclear receptor superfamily [13,14]. The three known PPAR isoforms, PPAR α , PPAR γ and PPAR δ , display isotype-specific target gene [15], ligand binding [16] and tissue distribution patterns [17]. PPAR γ regulates adipogenesis and is the target of the thiazolidinedione (TZD) class of insulin sensitizing drugs [18], while PPAR α regulates genes involved in hepatic fatty acid oxidation (FAO) [19] and lipoprotein metabolism [20] and is the molecular target of the fibrate class of dyslipidemia drugs [21]. PPAR δ is ubiquitously expressed and plays key roles in lipid metabolism, muscle fiber type composition and skin health [22,23,24]. Several chemical PPAR δ agonists exist [25], but none

are currently approved for use in humans. PPARs also have potent anti-inflammatory effects through transcriptional regulation of pro-inflammatory gene expression, both in the periphery [26] and central nervous system (CNS) [27].

All three PPAR isoforms are expressed to different degrees in the CNS [28]. Recent evidence suggests that CNS activation of PPAR α and/or PPAR γ may contribute to weight gain and obesity. Deletion of PPAR γ in neurons [29] or chemical inhibition of PPAR γ in the hypothalamus protects against the development of diet-induced obesity (DIO) [30]. Activation of this receptor with HF feeding or a chemical agonist increases weight gain [30], raising the possibility, at least, that HFD consumption activates neuronal PPAR γ as a pathogenic mechanism in obesity. Activation of hypothalamic PPAR α was also shown to correct the hypophagic phenotype in a model of increased CNS fatty acid sensing [31]. Although limited, this evidence supports a key role for PPARs in central energy homeostasis regulation.

PPAR δ is the most highly expressed isoform throughout the CNS and is enriched in areas known to be involved in energy homeostasis, such as mediobasal hypothalamus [28,32,33]. Accumulating evidence supports a role for CNS PPAR δ activation in preventing oxidative stress and inflammation in several neurodegeneration models [34,35]. Evidence from various rodent models suggests that hypothalamic lipid accumulation and low-grade inflammation are associated with obesity [9,12]. Given the known role of PPAR δ in the regulation of genes that promote lipid oxidation [22] and its recognized anti-inflammatory effects in the CNS [36], we hypothesized that loss of PPAR δ function, via genetic deletion, would lead to or potentiate obesity.

We generated neuronal PPAR δ knockout mice (KO) using Nest-Cre loxP technology [37]. Cre-mediated recombination leads to deletion of exon 4, which encodes the DNA binding domain of PPAR δ . On a chow diet, KO mice have increased fat mass, despite reduced body weight and lean mass. Elevated hypothalamic inflammation is accompanied by leptin resistance as well as abnormal feeding and neuroendocrine responses to fasting. Consistent with our hypothesis, KO mice are extremely susceptible to DIO, yet are surprisingly resistant to HF diet-induced elevations in CNS inflammation and lipid accumulation. Gene expression analysis revealed increased expression of genes of fatty acid oxidation and of the other PPARs with HF feeding, which may account for the lack of further increase in inflammation and lipotoxicity.

Results

Neuronal PPAR δ knockdown and brain morphology

In order to generate a neuronal loss-of-function PPAR δ allele, we crossed mice with a floxed PPAR δ allele [38] with mice expressing Cre recombinase under control of the rat nestin promoter [39]. Cre mediated recombination leads to excision of exon 4, which encodes the DNA binding domain of PPAR δ . Double heterozygous mice were crossed to Cre negative, homozygous floxed females to produce study animals. Heterozygous (Het) and homozygous neuronal PPAR δ knockout (KO) mice were born at the expected Mendelian ratios (not shown), were fertile and had no apparent developmental abnormalities compared to floxed littermate (f/f) control mice (not shown). PPAR δ mRNA expression in hypothalamus was reduced in a gene dosage dependent manner (Fig. 1A), but was not altered in peripheral tissues (muscle, liver, white and brown adipose; Fig. 1C). Western analysis revealed reduction of PPAR δ protein in mediobasal hypothalamus (Fig. 1B), although Western analysis for PPARs has proven technically difficult.

Because PPAR δ has been noted to have roles in brain development [24], we determined whether the CNS is grossly altered by deletion of the delta isoform. Nissl stain (Fig. 1D) of coronal sections at the level of the hippocampus (top panel) and hypothalamus (bottom panel) revealed no obvious differences or malformations in the structure of these or any other forebrain nuclei between KO mice and f/f “floxed” or nestin expressing unfloxed negative controls, indicating that deletion of PPAR δ in neurons does not cause major structural defects. Therefore, we proceeded to use this model to study the effects of loss of neuronal PPAR δ function in energy homeostasis.

Neuronal PPAR δ deletion leads to altered body composition and leptin insensitivity

Body weight (BW) of 5-week old, chow-fed KO mice ($n = 18-22$) was reduced by 13% (18.96 ± 0.33 vs. 16.85 ± 0.25 g, $p < 0.001$, t test), a difference that was largely due to a reduction in lean body mass (13.17 ± 0.35 vs. 11.16 ± 0.20 g, $p < 0.001$, t test). Lower body weight and slightly but significantly higher fat mass (1.47 ± 0.07 vs. 1.90 ± 0.05 g, $p < 0.001$, t test) in these animals resulted in a significant elevation in adiposity (fat mass/BW $\times 100$) (8.38 ± 0.48 vs. $12.22 \pm 0.32\%$, $p < 0.001$, t test).

The adipocyte hormone leptin acts as an adiposity negative feedback signal, controlling fat mass [3,40] through the coordinated regulation of food intake and energy expenditure. Resistance to the behavioral and biochemical effects of leptin is a hallmark of obesity [41]. Leptin treatment (5 mg/kg BW, i.p.) reduced 24 hour caloric intake, (kcal/g BW) by 24% in f/f mice (Fig. 2A) compared to vehicle, but failed to reduce food intake in KO mice (Fig. 2A). STAT3 is a direct, molecular target of leptin receptor activation [42] and its phosphorylation state can be used as a biochemical marker of leptin sensitivity. Leptin treatment (5 mg/kg BW, i.p.) significantly increased phosphorylation of STAT3 (Y705; Fig. 2B) in hypothalami of f/f mice, but this effect was significantly blunted in KO mice (Fig. 2B). These findings occurred in the context of a near doubling of epididymal adipose tissue (Fig. 2C) and higher circulating basal leptin levels (Fig. 2D), altogether suggesting that deletion of PPAR δ blunts leptin sensitivity in mediobasal hypothalamus.

Increased susceptibility to diet-induced obesity in KO mice

Based upon evidence that PPAR δ is activated by dietary fatty acids [43], we hypothesized that PPAR δ may be an important molecular determinant of susceptibility to environmentally induced obesity. To test this, we placed mice on a diet with high-fat (HF) content (45% kcal as fat, HFD) or a micronutrient match control diet with low-fat (LF) content (10% kcal as fat, LFD) at 5 weeks of age.

Although smaller at weaning, KO mice have normal growth and gain a similar amount of weight as f/f mice over 33 weeks of LFD feeding (Fig. 3A, D). On HFD, KO mice rapidly gain weight and become significantly heavier than KO mice fed LFD after 8 weeks and surpass the body weight of HFD fed f/f controls after 21 weeks on HFD (Fig. 3A). Ultimately KO mice gained 16% (~5 g, Fig. 3D) more body weight and were 6% heavier than f/f mice fed the same diet (Fig. 3A, Table 1), revealing a role for neuronal PPAR δ expression in the determination of body weight gain during HF feeding.

Differences in body composition can have profound effects on the metabolic implications of weight gain. On LFD, KO mice have lower lean mass (Fig. 3B, Table 1) and slightly reduced lean

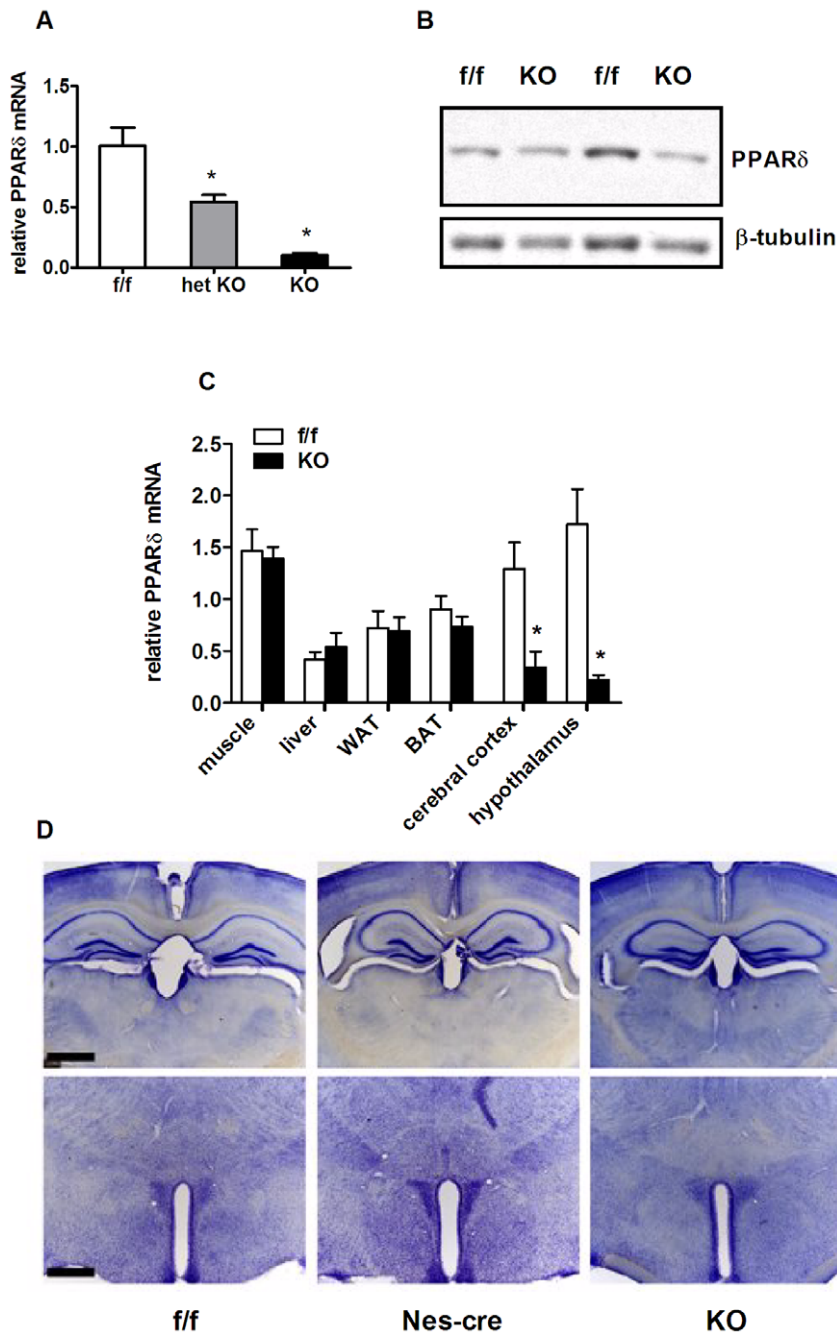


Figure 1. Neuronal PPAR δ knockdown and brain morphology. (A) PPAR δ gene expression in mediobasal hypothalamus of control (f/f), heterozygous KO (het) and homozygous KO (KO) PPAR δ mice. Target gene PPAR δ mRNA expression was measured by RT PCR and normalized to endogenous levels of the housekeeping gene RPL13A. (B) Representative Western blot of PPAR δ protein levels in total cellular protein extracts from mediobasal hypothalamus of f/f and KO mice. β -tubulin was used as a loading control. (C) Quantification of PPAR δ mRNA expression in peripheral and CNS tissues of f/f and KO mice (muscle, liver, white adipose tissue (WAT), brown adipose tissue (BAT), cerebral cortex and hypothalamus). Gene expression was measured by RT PCR and normalized to endogenous levels of the housekeeping gene RPL13A (n=4–8). (D) Photomicrographs of Nissl staining in brains from f/f, nestin cre+ control and KO mice. Representative sections shown at the level of the hippocampus (top) and hypothalamus (bottom). No obvious differences or malformations in the structure of these or any other forebrain nuclei were observed across genotypes. Scale bar = 500 μ m. Values in panels A and C represent the genotype group mean \pm SEM, expressed relative to the levels of the f/f control group. Statistical significance is designated as * ($p < 0.05$, vs. f/f control group, ANOVA or two-tailed student's *t* test). doi:10.1371/journal.pone.0042981.g001

mass gain (Fig. 3E), whereas HFD feeding lead to identical lean mass gain (Table 1).

At baseline, KO mice have slightly more fat mass (Fig. 3C, Table 1), and while on LFD, maintain a similar degree of elevated

fat mass over time (Fig. 3F). Consumption of HFD induces obesity in both groups, but the degree of DIO is augmented in the KO group. KO animals have 6 grams, or 33% more fat mass (Fig. 3C, F, Table 1), than HFD fed f/f mice. Thus, increased body weight

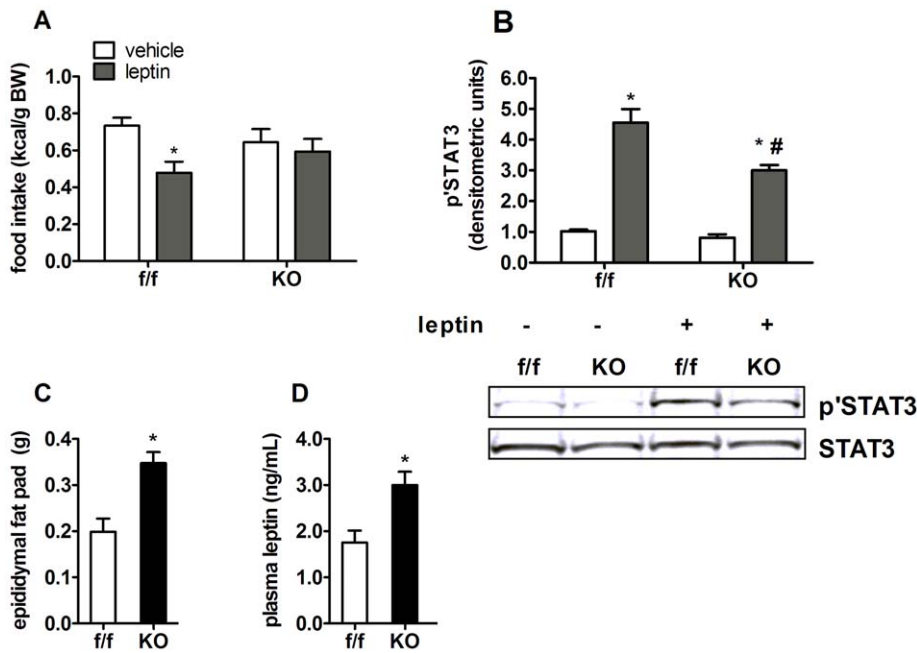


Figure 2. Neuronal PPAR δ deletion leads to leptin insensitivity. (A) Food intake in chow fed *f/f* and KO mice after receiving a bolus injection of leptin (5 mg/kg BW, i.p.) or vehicle (saline) at the onset of the dark period. Mice were housed individually and food intake was measured over 24 hours ($n=10-12$). (B) Hypothalamic total protein extracts from *f/f* and KO mice treated with leptin (5 mg/kg BW i.p.) or vehicle for 30 minutes were used for Western blot analysis to detect levels of STAT3 phosphorylation (Y705). Total STAT3 levels were determined and used as a loading control. Densitometry of blots yielded relative intensity of protein levels, which are expressed as an activation index (pSTAT3/total STAT3) and represented as the group mean \pm SEM ($n=4-6$) relative to the *f/f* saline group. (C) Epididymal fat pad mass and (D) plasma leptin levels of aged matched, chow fed *f/f* and KO mice represent basal phenotype of these mice. Values represent the mean \pm SEM. Statistical significance is denoted in A and B as * ($p<0.05$ leptin (gray bars) vs. vehicle (white bars) treated groups within each mouse genotype) or # ($p<0.05$, KO vs. *f/f* mice treated with leptin), and in panels C and D as * ($p<0.05$ vs. *f/f* controls, two-tailed student's *t* test). doi:10.1371/journal.pone.0042981.g002

gain in KO mice on HFD is due to a profound accumulation of fat mass. These data reveal a significant interaction between CNS PPAR δ and dietary fat exposure in DIO.

Impact of Neuronal PPAR δ deletion on food intake and energy expenditure

Impaired neuroendocrine regulation of energy balance leads to obesity. Absolute food intake was reduced in KO mice on LFD, whereas no differences in cumulative food intake were observed on HFD (Fig. 3G). Feed efficiency (calculated as the number of consumed calories required to gain 1 gram of mass) was elevated for body weight gain on HFD, and for fat mass gain on both LFD and HFD, in KO mice relative to controls (Fig. 3H, I). Interestingly, feed efficiency for lean mass gain was not different in control mice on either diet (Fig. 3H, I). Together these data suggest that KO mice are more efficient at storing calories as fat.

To determine if reduced energy expenditure contributes to increased fat mass gain in KO mice, we measured energy expenditure (EE) by indirect calorimetry. Interestingly, after 20 weeks of HFD exposure, daily EE (kcal) and EE normalized to total body weight (kcal/g BW) were not different in KO mice relative to *f/f* mice (Table 2). At this time point, KO animals had similar total body weight (Fig. 1A, Table 2) but reduced lean mass (Fig. 1B, Table 2) relative to controls. When normalized per gram lean mass (kcal/gram lean body mass), KO mice exhibit a slight but significant elevation in EE over 24 hours, relative to *f/f* mice (Table 2). During the measurement period, both total food intake (kcal/day) and food intake normalized to body weight (kcal/day/gram BW) in KO mice were similar to that of *f/f* controls. When

food intake was normalized to lean mass (kcal/day/gram lean mass), KO mice exhibited increased intake (Table 2).

Consistent with elevated adiposity, KO mice had significantly higher plasma leptin levels on chow diet (Fig. 2D) and on both LFD and HFD (Table 1). Insulin was also elevated in KO mice (Table 1), but only on HFD, and was accompanied by modest effects on glucose tolerance (area under the glucose curve; AUC, Fig. S1A, B) on both LFD and HFD. The stress hormone corticosterone is associated with elevated adiposity and insulin resistance; nadir, peak and stress induced plasma corticosterone levels were not altered in KO mice (Fig. S1C), ruling out gross abnormalities in the hypothalamic-pituitary-adrenal axis as a cause for elevated fat mass gain.

Effects of dietary fat and PPAR δ deletion on brain lipids, fatty acid composition, and lipid metabolism genes

Hypothalamic lipid accumulation/lipotoxicity is implicated in obesity [9]. On a LFD, loss of PPAR δ did not alter total brain lipid (free fatty acid (FFA), diglyceride (DG), triglyceride (TG)) content (Fig. 4A). On HFD, in control animals, total brain FFA levels were increased by 1.5-fold, while conversely, KO animals displayed no change in brain FFA levels relative to LFD (Fig. 4A) and were lower than controls on HFD. In order to identify a potential transcriptional mechanism, we assessed the expression level of genes involved in lipid uptake (lipoprotein lipase (LPL) and cluster of differentiation 36 (CD36)) and triglyceride storage (glycerol-3-phosphate acyltransferase (GPAT) and diacylglycerol acyltransferase (DGAT)). On LFD, gene expression of LPL, CD36 and DGAT were similar between *f/f* and KO groups, while GPAT

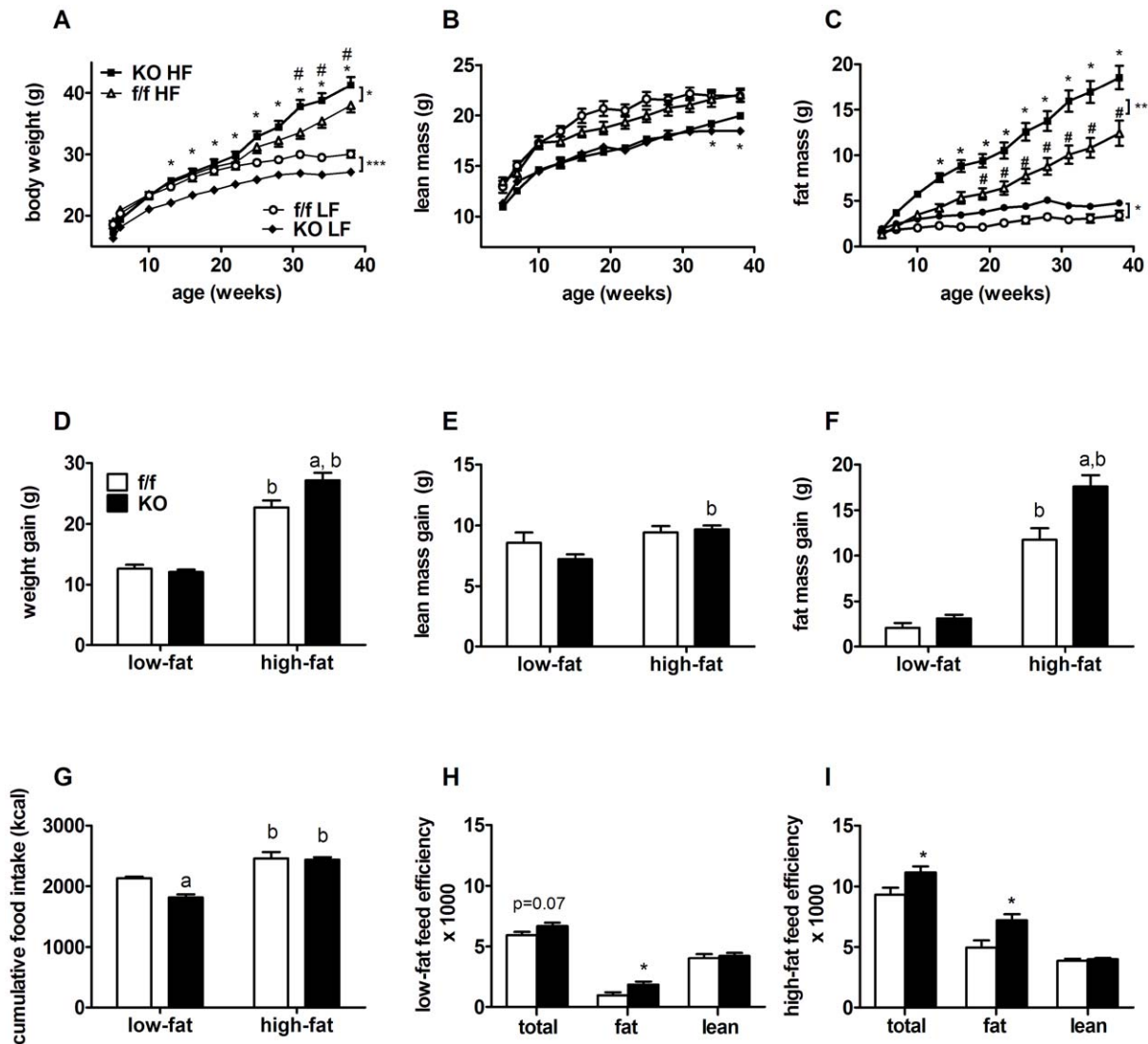


Figure 3. Neuronal PPAR δ deletion leads to increased susceptibility to diet induced obesity. Growth curves of f/f and KO mice fed LFD or HFD for 33 weeks (age 5–38 weeks). Body weight (BW) and body composition (fat and lean mass) were measured at the indicated ages by MRI/NMR. (A) BW curves, (B) lean mass curves, (C) fat mass curves. Susceptibility to diet-induced obesity was measured by two-way repeated measures ANOVA over the experimental period (*, $p < 0.05$, f/f mice fed LF vs. HF diet) and (#, $p < 0.05$, KO mice fed LF vs. HF diet). Total weight gain over the experimental period for (D) body weight gain, (E) lean mass gain, (F) fat mass gain are shown for f/f and KO mice. (G) Cumulative food intake (kcal) of f/f and KO groups fed either LF or HF diets for 33 weeks, determined from bi-weekly measurements of food intake in genotype matched, group housed mice. Feed efficiency of f/f and KO mice fed (H) LFD and (I) HFD is the ratio of weight gained (BW, fat and lean) to that of calories consumed over the entire study period. Values represent the mean \pm SEM. Statistical significance is denoted by ^a ($p < 0.05$, f/f vs. KO, same diet) or ^b ($p < 0.05$, LF vs. HF, same genotype), as determined by one-way ANOVA and Bonferroni post test, or by * ($p < 0.05$ vs. f/f controls), when determined by two-tailed student's *t* test.

doi:10.1371/journal.pone.0042981.g003

expression was increased by 2.4-fold in KO mice on LFD relative to LFD controls (Fig. 4B). KO mice expressed higher levels of LPL and CD36 on HFD, compared to HFD fed f/f control mice (Fig. 4B), while DGAT expression did not change (Fig. 4B). GPAT expression did not change in HFD fed KO mice, relative to LFD fed, however on HFD, was no longer significantly elevated above controls (Fig. 4B).

Levels of individual FFA species were similar between genotypes on LFD (Fig. 4C). In f/f control animals, HFD increased the prevalence of saturated FFAs, palmitate (16:0) by 1.5-fold and stearate (18:0) by 1.4-fold, and the monounsaturated FFA oleate (18:1) by 1.2-fold (Fig. 4C). PPAR δ deletion prevented a further accumulation of these common dietary FFAs in the CNS on HFD,

relative to LFD (Fig. 4C). To determine if lipogenesis contributed to elevations in FFA levels in f/f mice, gene expression of the key lipogenic enzymes, fatty acid synthase (FAS) and acetyl-CoA carboxylase (ACC), as well as stearoyl CoA desaturase 1 (SCD1) were determined. On LFD, FAS expression was 3.1-fold higher in KO mice compared to f/f mice. HFD increased FAS in f/f mice (Fig. 4D), but did not alter expression in KO mice. Expression of SCD1 was also elevated by 2.4-fold in KO mice on LFD, compared to f/f mice. On HFD, SCD1 expression was not different between the groups. Gene expression of ACC was similar between the groups (Fig. 4D).

In agreement with increased expression of FAS, GPAT and SCD1, KO mice had elevated triglyceride levels composed of 18:1

Table 1. Plasma hormones and metabolites after 33 weeks of low-fat (LFD) or high-fat (HFD) diet.

	LFD (10% kcal fat)		HFD (45% kcal fat)	
	f/f	KO	f/f	KO
body weight (g)	29.94 \pm 0.58	27.11 \pm 0.38 ^a	39.56 \pm 0.72 ^b	42.07 \pm 1.20 ^{a,b}
fat mass (g)	3.40 \pm 0.53	4.76 \pm 0.38 ^a	13.27 \pm 1.18 ^b	18.55 \pm 1.29 ^{a,b}
lean mass (g)	21.90 \pm 0.59	18.47 \pm 0.28 ^a	21.16 \pm 0.34	19.95 \pm 0.30
insulin (ng/mL)	0.61 \pm 0.08	1.00 \pm 0.15	1.26 \pm 0.26	2.21 \pm 0.20 ^{a,b}
leptin (ng/mL)	5.7 \pm 1.0	18.1 \pm 2.3 ^a	64.7 \pm 21.4 ^b	129.3 \pm 11.4 ^{a,b}
FFA (mM)	0.66 \pm 0.08	0.63 \pm 0.06	0.82 \pm 0.08	0.73 \pm 0.03
TG (mg/dL)	38.1 \pm 3.0	53.09 \pm 5.2 ^a	63.6 \pm 5.5 ^b	46.5 \pm 4.2

Metabolic characteristics, plasma hormones and metabolites were measured after 33 weeks of HFD or LFD feeding. Body composition was measured by NMR. Insulin and leptin levels were measured by RIA. FFA and TG were quantified as described in methods and materials. Mice were fasted for 4 hours prior to plasma collection. Values represent group mean \pm SEM (n=9–11) and statistical significance is designated by a (p<0.05, f/f vs. KO, same diet) or b (p<0.05, LFD vs. HFD, same genotype), as determined by two-way ANOVA followed by Bonferroni post test.

doi:10.1371/journal.pone.0042981.t001

on LFD (Fig. 4E). Transition to a HFD resulted in significantly reduced levels of TG composed of 16:0 in KO animals, while HFD led to reduced 18:1 in TG of f/f mice but did not alter other TG lipid species (Fig. 4E). We next assessed gene expression of key genes involved lipid catabolism to determine if increased fatty acid oxidation might contribute to decreased lipid accumulation in brains of KO mice on HFD. On LFD, pyruvate dehydrogenase kinase 4 (PDK4) expression was increased by 1.7-fold in KO mice (Fig. 4F). HFD led to increased expression of the mitochondrial uncoupling gene uncoupling protein 2 (UCP2) in f/f mice by 2.4-fold, but did not alter UCP2 expression in KO mice (Fig. 4F). On HFD, KO mice had higher gene expression (2-fold) of two markers of mitochondrial fatty acid oxidation, carnitine palmitoyl-transferase 1A (CPT1A) and PDK4 compared to f/f mice on HFD. Gene expression of acyl-CoA oxidase (ACO), a marker of peroxisomal fatty acid beta-oxidation, was not different among the groups on either diet (Fig. 4F). As a whole, these data suggest that PPAR delta could play important regulatory roles in basal CNS lipid homeostasis and responses to dietary lipid exposure.

Gene-diet interactions determine hypothalamic inflammatory signaling and gene expression in neuronal PPAR δ KO mice

Activation of PPAR δ has anti-inflammatory effects in both the periphery and CNS [34,44]. In order to determine if loss of PPAR δ increases inflammatory signaling in hypothalamus, we measured levels of the cytoplasmic inhibitory protein of NF- κ B, I κ B α , and the pro-inflammatory cytokines, IL-6 and IL-1 β , which are two transcriptional targets of NF- κ B [45]. Interestingly, I κ B α levels in hypothalamic total cell extracts were reduced by 25% in KO mice fed LFD, compared to LFD fed f/f mice (Fig. 5A). In response to dietary fat exposure, I κ B α levels were reduced by ~40% (Fig. 5A) in f/f hypothalami, as reported in several models and is consistent with lipotoxicity and activation of pro-inflammatory signaling [9,10]. Interestingly, HFD feeding in KO animals failed to further reduce I κ B α protein levels (Fig. 5A). An identical response was observed for I κ B α mRNA levels (Fig. 5B). Consistent with I κ B α data, KO animals have increased hypothalamic

Table 2. Energy homeostasis analysis after 20 weeks of high-fat diet (HFD) exposure.

	f/f	KO
	BW (g)	30.10 \pm 1.44
lean mass (g)	19.05 \pm 0.37	16.95 \pm 0.42 ^{**}
Daily EE (kcal)	11.11 \pm 0.18	11.01 \pm 0.27
Daily EE (kcal/g BW)	0.38 \pm 0.01	0.35 \pm 0.01
Daily EE (kcal/g lean mass)	0.58 \pm 0.01	0.65 \pm 0.01 ^{**}
RER light period	0.91 \pm 0.01	0.86 \pm 0.01
RER dark period	0.86 \pm 0.01	0.82 \pm 0.02
Daily FI (kcal)	10.78 \pm 0.24	10.43 \pm 0.62
Daily FI (kcal/g BW)	0.37 \pm 0.01	0.37 \pm 0.01
Daily FI (kcal/g lean mass)	0.58 \pm 0.02	0.64 \pm 0.02 ^{**}

Energy expenditure (EE) and respiratory exchange ratio (RER) were measured over 24 hours by indirect calorimetry in individually housed f/f and KO mice after 20 weeks on HFD (n=4). Values for EE (kcal/hour) and food intake were also normalized to body weight and lean body mass measured by NMR. Mean \pm SEM,

*p<0.05,

**p<0.01,

***p<0.001 KO vs. f/f same diet, Student's t test.

doi:10.1371/journal.pone.0042981.t002

IL-6 gene expression on LFD relative to controls (Fig. 5C). While HFD increased IL-6 gene expression, and another NF- κ B target pro-inflammatory gene, IL-1 β , in f/f controls, KO animals were protected from further HFD induced increases in hypothalamic inflammatory cytokine gene expression (Fig. 5C, D).

Adipose tissue hypertrophy and inflammation

Adipose tissue serves as a source of circulating cytokines that promote systemic inflammation in obesity. Adipose inflammation, measured by the presence of crown-like structures (CLS) corresponding to macrophage infiltration (Fig. 6A, B), and TNF α mRNA expression (Fig. 6C), were similarly elevated in epididymal white adipose tissue (WAT) from f/f and KO mice on HFD. Increased adiposity is accompanied by adipose hypertrophy in KO mice on chow diet (Fig. 6A), but there were no differences in WAT expression of the adipogenic markers PPAR γ (Fig. 6D) and LPL (Fig. 6E). Collectively, these data suggest that alterations in adipocyte function or systemic inflammatory status do not explain changes (or lack thereof) in CNS inflammation in KO mice fed HFD.

Neuronal PPAR δ deletion alters regulation of hypothalamic neuropeptide gene expression and responses to prolonged fasting

To identify mechanisms by which loss of neuronal PPAR δ increases DIO susceptibility, we measured hypothalamic mRNA expression of key regulatory neuropeptides, NPY and POMC, following HFD and LFD feeding. On LFD, NPY expression was increased by 1.8-fold in KO mice (Fig. 7A). HFD feeding led to a 2-fold increase in NPY expression in f/f mice, but had no effect to further increase NPY in KO mice (Fig. 7A). POMC expression was not different on LFD between KO and controls (Fig. 7B). HFD increased POMC expression by 2.4-fold in f/f mice relative to LFD, but did not alter POMC in KO animals on HFD relative to LFD (Fig. 7B) despite a ~3-fold increase in circulating leptin levels (Table 1). Collectively, these data suggest profound dysregulation of adiposity negative feedback signaling and

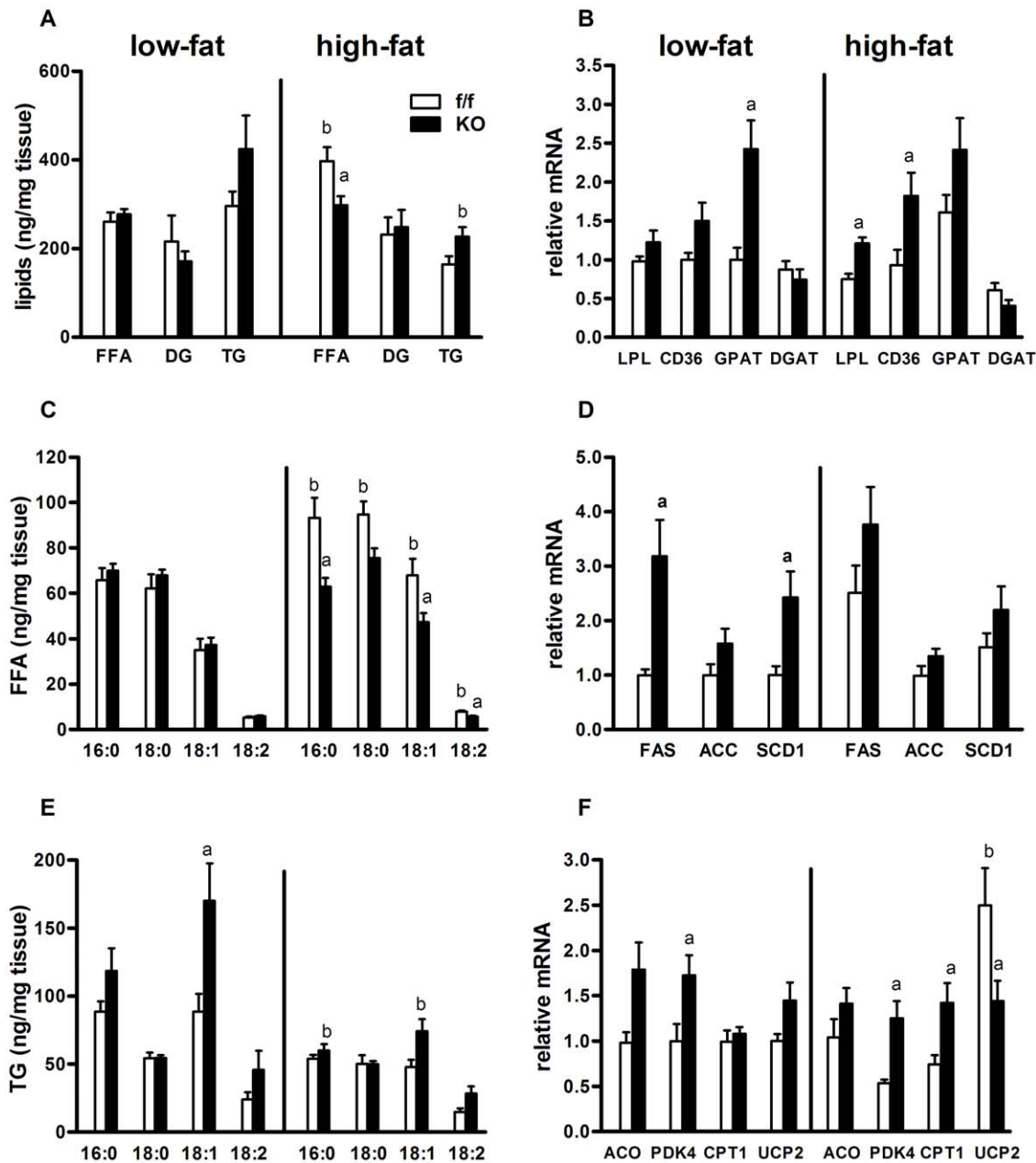


Figure 4. Effects of dietary fat and PPAR δ deletion on brain lipids, fatty acid composition and lipid metabolism genes. (A) Total levels of triglyceride (TG), diglyceride (DG) and free fatty acid (FFA) extracted from total lipids from brains of *f/f* and KO mice fed LFD or HFD for 33 weeks ($n=6-7$). Composition of individual FFA species making up the (C) FFA and (E) TG fractions were determined by GC-MS analysis, normalized to brain tissue mass (ng/mg tissue) and shown as group mean \pm SEM. (B) Changes in hypothalamic mRNA levels of target genes involved in (B) lipid uptake and storage (LPL, CD36, GPAT and DGAT), (D) lipid synthesis (FAS, ACC, SCD) and (F) fatty acid oxidation (ACO, PDK4, CPT1A, UCP2) were assessed by quantitative real-time PCR. Gene expression levels were normalized to endogenous RPL13A levels and are expressed as group mean \pm SEM relative to the level of the *f/f* LF diet control group. Statistical significance is designated as ^a ($p<0.05$, *f/f* vs. KO, same diet) or ^b ($p<0.05$, LF vs. HF, same genotype), as determined by one-way ANOVA and Bonferroni post test. doi:10.1371/journal.pone.0042981.g004

regulation of neuropeptide gene expression in KO mice on both diets.

The orexigenic neuropeptide NPY is a powerful activator of food intake. NPY expression is potently induced by fasting and in the absence of leptin signaling [46]. In this situation, simultaneous inhibition of POMC neurons (and down regulation of anorexogenic POMC gene expression) facilitates subsequent hyperphagia and weight regain. Fasting elicited the appropriate neuropeptide

expression pattern in hypothalamus of *f/f* mice, increasing NPY by 1.8-fold (Fig. 7C) and decreasing POMC expression by half (Fig. 7D). Fasting paradoxically decreased NPY expression in KO mice (Fig. 7C) and did not lead to reduction of POMC expression (Fig. 7D). UCP2, a known target of PPAR δ regulation, has been implicated in hypothalamic nutrient sensing, and neuronal responsiveness to changes in energy availability and adiposity negative feedback signaling [47]. UCP2 expression was increased

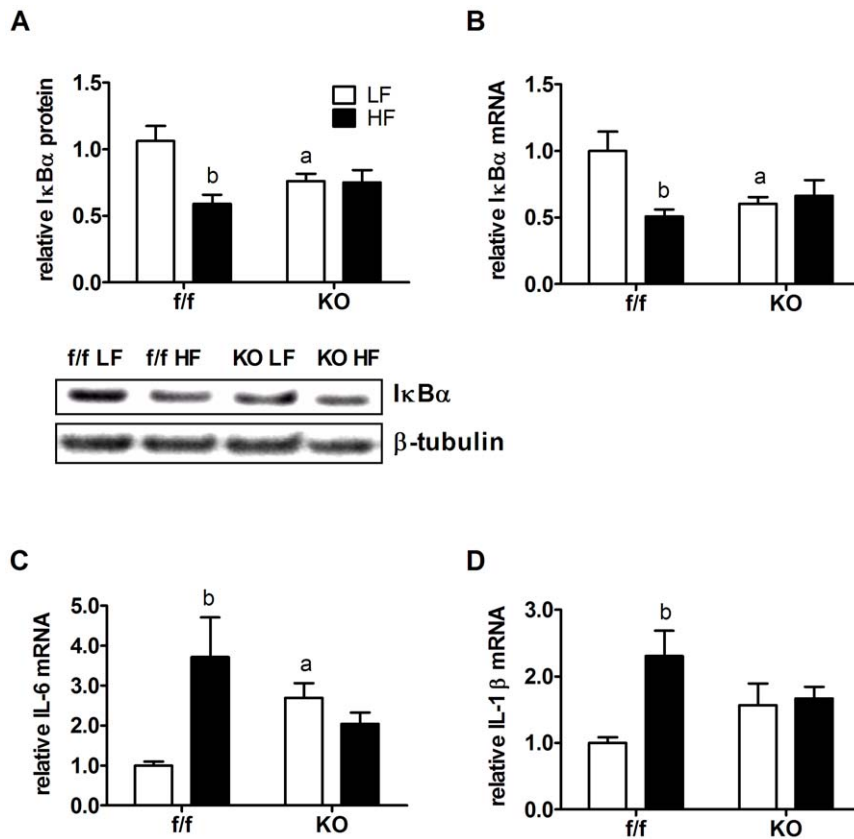


Figure 5. Gene-diet interactions determine hypothalamic inflammatory signaling and gene expression in neuronal PPAR δ KO mice. Protein and mRNA were isolated from bisected sections of mediobasal hypothalamus of *f/f* and KO mice fed LFD or HFD for 33 weeks. (A) Total hypothalamic protein extracts were subjected to Western blot analysis using an antibody directed against I κ B α . Levels of β -tubulin were determined and used as a loading control. Densitometry of blots yielded relative intensity of protein levels ($n=6$). Insert of A shows a representative Western blot. Hypothalamic mRNA levels of (B) I κ B α and inflammatory cytokines (C) IL-6 and (D) IL-1 β in *f/f* and KO mice measured by RT-PCR after the study period. Target gene mRNA levels were normalized to endogenous RPL13A levels. Values are represented as group mean \pm SEM relative to the LF *f/f* control group. Statistical significance is designated by ^a ($p<0.05$, *f/f* vs. KO, same diet) or ^b ($p<0.05$, LF vs. HF, same genotype), as determined by two-way ANOVA and Bonferroni post test. doi:10.1371/journal.pone.0042981.g005

1.6-fold by fasting (Fig. 7E) in *f/f* mice but was unchanged in KO mice, suggesting a potential molecular mechanism for disruption of neuropeptide gene expression.

To understand the functional implications of altered neuropeptide expression in KO mice, we measured food intake in a second group of individually housed mice following a 24 hour fast. Consistent with blunted fasting induced UCP2 and NPY expression, KO mice consumed significantly fewer calories (normalized to lean mass, kcal/g lean mass) after fasting (Fig. 7F), resulting in attenuated weight regain after 24 hours of refeeding (Fig. 7G). Interestingly, KO mice gained significantly more weight than *f/f* mice in the 8 days following the fasting challenge (Fig. 7G), suggesting that stress-induced weight gain may be exaggerated in the longer term. Together with impaired leptin sensitivity, these data raise the possibility that loss of PPAR δ function in neurons impairs both anorexigenic and orexigenic tone.

Neuronal PPAR δ deletion leads to increased hypothalamic PPAR γ and PPAR α expression

We next evaluated hypothalamic expression of all the PPAR isoforms to determine if PPAR α and PPAR γ could be involved in variations in brain lipid content and gene expression in KO mice. Gene deletion of PPAR δ resulted in a \sim 90% reduction of mRNA expression, on both diets (Fig. 8A). Expression of PPAR α and

PPAR γ were similar between *f/f* and KO mice fed LFD (Fig. 8). Consumption of HFD increased PPAR α expression by 1.6-fold in KO mice relative to LFD fed mice, but not relative to HFD fed *f/f* mice (Fig. 8). Potentially consistent with reduced CNS FFA accumulation in KO mice on HFD (Fig. 4C), expression of the PPAR α target gene, CPT1A, was increased, although expression levels of another target gene, ACO, was not different between genotypes (Fig. 4F). PPAR γ expression was 2.6-fold higher in KO mice than *f/f* mice on HFD (Fig. 8), a finding that is potentially consistent with reduced hypothalamic inflammatory tone (Fig. 7) and elevated expression of the PPAR γ target genes, LPL and CD36 (Fig. 4B), in KO animals on HFD.

Discussion

Dietary fat contributes to obesity pathogenesis independent of caloric density [48]. Lipotoxicity and inflammation in key regulatory neurons and brain regions (such as mediobasal hypothalamus) are thought to contribute to positive energy balance and weight gain [9,10,12]. PPAR δ regulates transcription of genes involved in fatty acid oxidation and has been shown to reduce inflammation and promote insulin sensitivity in peripheral tissues [22,49,50]. Relatively less is known about PPAR δ function in the CNS where it has been implicated in neuroprotection by

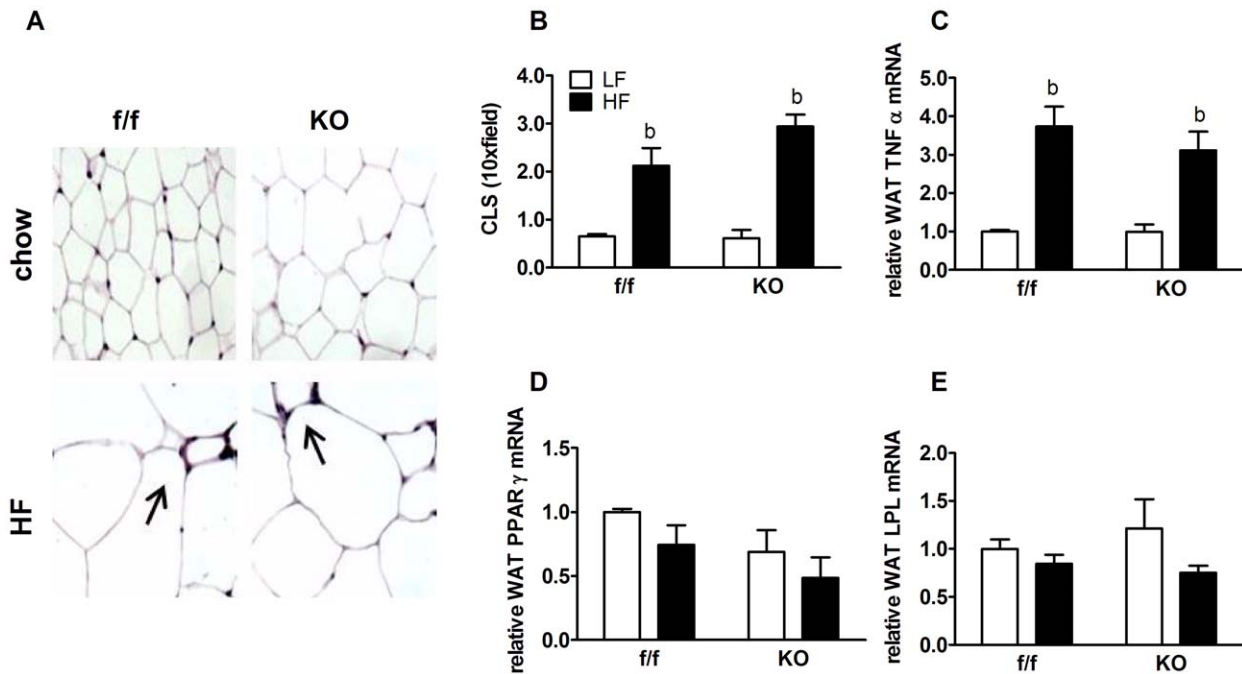


Figure 6. White adipose tissue hypertrophy and inflammation. (A) Light micrographs ($\times 10$ magnification) of H&E stained slides of WAT from f/f and KO mice fed chow or HFD for 33 weeks. Arrows point to crown-like structures (CLS), of areas of macrophage infiltration and inflammation. (B) Quantification of CLS (CLS/10 \times field, $n = 4$) corresponding to inflammatory macrophage infiltration around adipocytes in f/f and KO mice fed either a chow diet or a HFD. Adipose gene expression of inflammatory cytokine (C) TNF α and adipogenesis markers (D) PPAR γ and (E) LPL measured by RT PCR. Target gene mRNA levels were normalized to endogenous RPL13A levels. Values are represented as group mean \pm SEM relative to the f/f LF group. Statistical significance is designated as ^b ($p < 0.05$, LF vs. HF same genotype), as determined by two-way ANOVA and Bonferroni post test. doi:10.1371/journal.pone.0042981.g006

opposing neuronal inflammation and oxidative stress (reviewed in [36]). We sought to identify a role for neuronal PPAR δ in energy homeostasis, and hypothesized that PPAR δ acts to reduce lipid accumulation and inflammation, opposing the development of biochemical resistance to homeostatic signals such as leptin. Thus, neuronal deletion, we hypothesized, would lead to obesity. Consistent with this hypothesis, neuronal PPAR δ deletion results in a profound susceptibility to DIO.

Interestingly, we also observed increased adiposity on LFD. The baseline phenotype is characterized by increased fat mass, lower lean mass and elevated feed efficiency on a LFD (Fig. 3, Table 1). Given the primary role of leptin in the regulation of energy balance [51], it was not surprising that KO animals exhibit blunted behavioral (Fig. 2A) and signaling responses (Fig. 2B) to leptin stimulation. These findings on LFD suggest that PPAR δ plays an important role in energy homeostasis regulation, even in the absence of excess dietary fat. On a HFD, genetic loss of PPAR δ function further potentiated fat mass gain (Fig. 3C), consistent with our hypothesis that PPAR δ mediates protective effects against a lipotoxic environment. Interestingly, excess fat mass accrual occurred in the absence of large differences in food intake or energy expenditure (normalized to either BW or lean mass). Therefore, preferential disposition of consumed calories towards adipose tissue storage, likely coupled with subtle imbalances between food intake and energy expenditure, contributes to excess adiposity and weight gain in these animals over time. Deletion of the melanocortin-3 receptor, results in a similar fuel partitioning phenotype [52].

Given its role in the transcriptional regulation of lipid metabolism, we hypothesized that deletion would potentiate the effects of HFD on CNS lipid accumulation. Instead, neuronal PPAR δ deletion did not promote lipid accumulation and opposed

accumulation of FFAs in the brain of KO mice fed a HFD, despite increased expression of two genes involved in cellular lipid uptake, LPL and CD36 (Fig. 4B). The lack of rise of FFA content may be related to the relative overexpression (compared to control animals) of fatty acid oxidation genes in hypothalamus, including CPT1 and PKD4 (Fig. 4F). Brain TG content was modestly reduced in both null and control animals on HFD (Fig. 4A, E), consistent with a reduction in expression of DGAT, an enzyme required for TG synthesis. Thus, at face value, these findings in the CNS contradict the general concept that PPAR δ activation opposes lipid accumulation, at least the species we measured. In reality, PPAR δ utilizes several modes of transcriptional regulation and can repress basal transcription of target genes when not ligand bound, while other genes, including UCP2, do not appear to be repressed and are not upregulated by PPAR δ depletion [53,54]. Indeed, it has been demonstrated in macrophages in vitro [55] and in cardiac tissue in vivo [56] that depletion of PPAR δ has a similar effect as ligand induced activation, to increase expression of some fatty acid oxidation genes [53]. In this context, genetic deletion ultimately leads to de-repression, which is consistent with the observed upregulation of PDK4, a target gene involved in fatty acid oxidation, in our KO model (Fig. 4F).

Interestingly, despite little change or a relative reduction in brain lipids, KO animals exhibited elevated markers of hypothalamic inflammation on LFD. Surprisingly, KO animals were resistant to further activation of hypothalamic inflammation in response to HFD (Fig. 5). This was true whether we assessed I κ B α , a key upstream regulator of NF- κ B activity, or IL-6 and IL-1 β , two key pro-inflammatory targets of NF- κ B regulation. These effects could not be attributed to alterations in peripheral inflammatory mediators, as KO and control adipose tissue exhibited similar levels of markers of inflammation (Fig. 6),

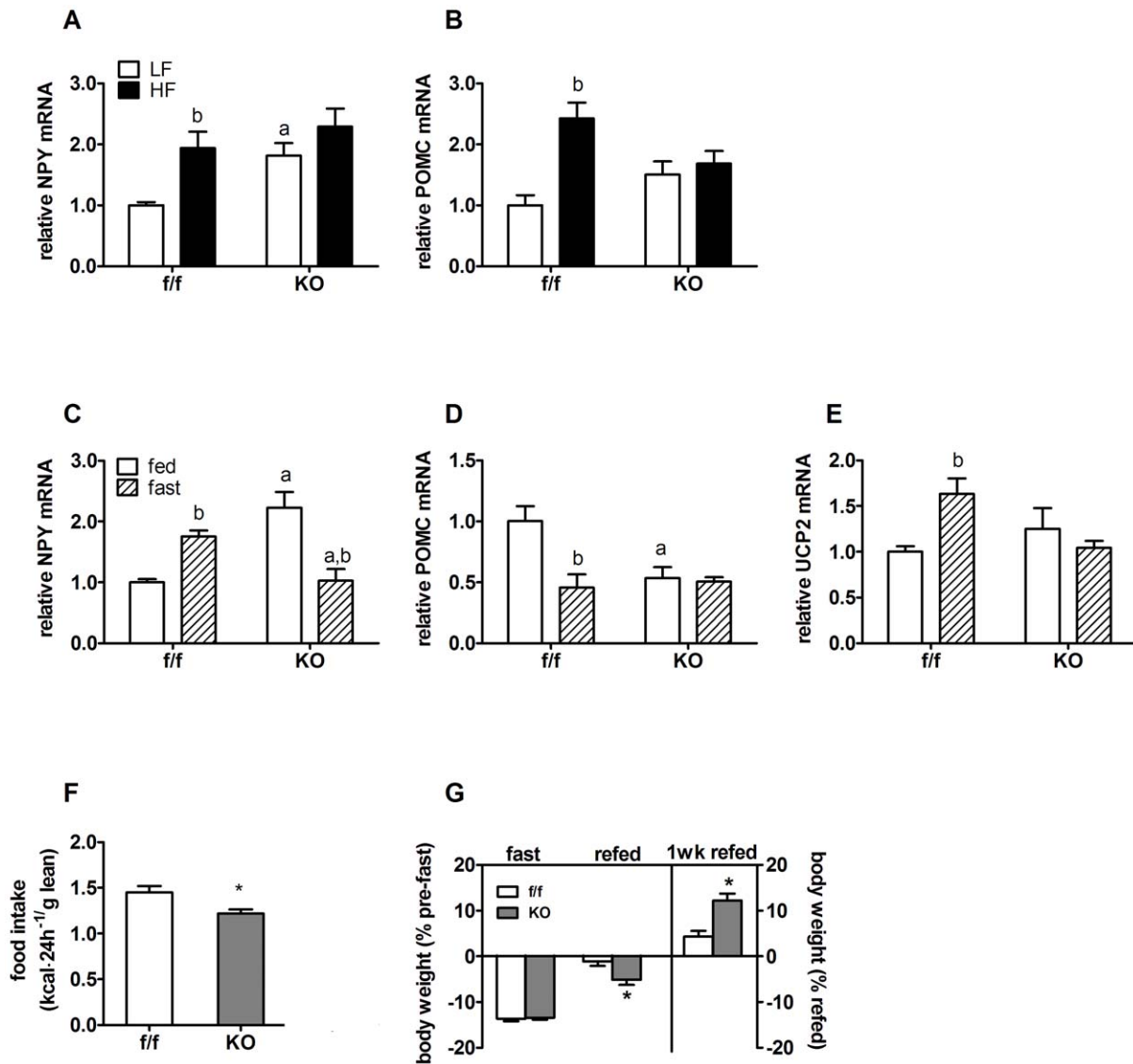


Figure 7. Neuronal PPAR δ deletion alters hypothalamic neuropeptide gene expression and compensatory hyperphagia after prolonged fasting. Hypothalamic mRNA levels of neuropeptides in *f/f* and KO mice fed LFD or HFD for 33 weeks ($n = 6-7$). Target gene mRNA levels of (A) NPY and (B) POMC were assessed by quantitative RT PCR. (C-D) Fasting induced changes in hypothalamic neuropeptide mRNA levels of *f/f* and KO mice maintained on a chow diet or fasted for 24 hours. Target gene mRNA levels of (C) NPY, (D) POMC and (E) UCP2 in fed and fasted mice were normalized to RPL13A and are expressed relative to the *f/f*, fed control. (F) Refeeding after fasting was measured for an additional 24 hours in a separate cohort of individually housed chow fed mice ($n = 6-7$). Graph shows food intake normalized to basal, pre-fast lean mass (kcal/g lean mass). (G) Percent changes in body weight after a 24 hour fast, after fasting and refeeding for 24 hours, or an additional 7 days. Values represent the mean \pm SEM. Statistical significance in panel A-E is designated as ^a ($p < 0.05$ *f/f* vs. KO, same diet) or ^b ($p < 0.05$, LF vs. HF, same genotype), as determined by two-way ANOVA and Bonferroni post test, and in F and G by * ($p < 0.05$ vs. *f/f*), as determined by two-tailed student's *t* test. doi:10.1371/journal.pone.0042981.g007

however, the lack of accumulation of saturated fatty acids (and presumably of lipotoxic intermediaries) may explain this. Further, PPAR δ is known to interact with and sequester the nuclear corepressor and negative regulator of NF- κ B, BCL-6, which is released upon ligand binding or loss of PPAR δ [57].

Consistent with hypothalamic dysfunction indicated by impaired leptin responses, KO animals exhibited marked abnormalities in compensatory responses to fasting and refeeding (Fig. 7C). These findings raise the possibility of impaired stress responses, however there were no differences in baseline, nadir, or stressed levels of corticosterone (Fig. S1C). Dramatic differences in neuropeptide gene expression (both NPY and POMC) at baseline,

and a complete absence of compensatory responses to fasting (Fig. 7C, D) and HFD (Fig. 7A, B), further suggest profound dysregulation of energy balance.

Interestingly, the blunted fasting induced UCP2 and NPY expression and impaired refeeding response in our neuronal KO model were similar to a global PPAR δ KO model [58]. An explanation for neuropeptide dysregulation could be blunted fasting or HFD induced UCP2 expression and augmented reactive oxygen species (ROS) production. ROS serve as nutrient signals and second messengers in hypothalamic neurons, where they are known to repress NPY while simultaneously promoting POMC expression [59]. The regulatory effects of ROS to repress NPY

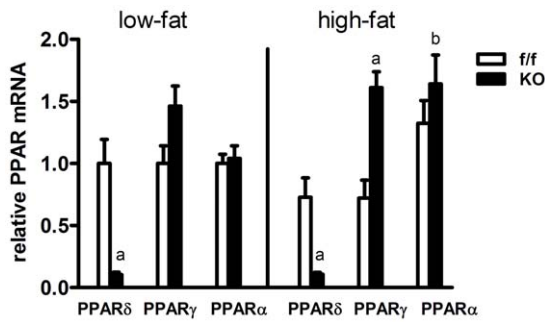


Figure 8. Effects of neuronal PPAR δ deletion on hypothalamic PPAR γ and PPAR α expression. Hypothalamic mRNA expression of PPAR isoforms in f/f and KO mice fed LFD or HFD for 33 weeks was assessed by quantitative real-time PCR. Changes in PPAR δ , PPAR γ and PPAR α were normalized to endogenous RPL13A levels and expressed relative to that of the f/f LFD group. Values represent group mean \pm SEM (n = 6–7). Statistical significance is designated ^a ($p < 0.05$, f/f vs. KO, same diet) or ^b ($p < 0.05$, LF vs. HF, same genotype), as determined by two-way ANOVA and Bonferroni post test. doi:10.1371/journal.pone.0042981.g008

neuronal activation and neuropeptide expression are abrogated by UCP2 mediated mitochondrial uncoupling [47]. Mice that overexpress UCP2 have elevated NPY expression but also exhibit reduced basal inflammation [60]. Conversely, mice lacking the gene for UCP2 have elevated levels in peripheral tissues of basal NF- κ B activation [61] and increased cytokine expression after ischemic injury [62]. UCP2 also protects against hypothalamic injury and inflammation [63]. Although KO mice display a slight increase in basal UCP2 expression (Fig. 4F), fasting and HFD feeding failed to further increase UCP2 expression, which was associated with elevated basal inflammatory cytokine gene expression (Fig. 4 and 7).

In addressing mechanisms involved in lipid metabolism and inflammation, we observed consistent changes in the expression of several isoform specific target genes (Fig. 4) of PPAR α (CPT1A) and PPAR γ (LPL) [30,64]. Indeed, PPAR α expression was slightly elevated, while PPAR γ was significantly elevated in brains of KO mice on HFD (Fig. 8). Two additional target genes of PPAR γ , CD36 and GPAT, were also elevated in KO mice (Fig. 4). Deletion of PPAR δ in cardiomyocytes, and in vitro systems, was shown to cause a similar induction of PPAR α , PPAR γ and their target genes involved in fatty acid oxidation [53,56,65]. Activation of hypothalamic PPAR α and/or PPAR γ has been implicated in weight gain and obesity, potentially consistent with elevated adiposity and DIO in PPAR δ KO mice. Given multiple complex modes of regulation of multiple target genes, including other PPAR isoforms [54,66], an understanding of the relevance of PPAR α and PPAR γ upregulation will require further study with more specific tools across a broader range of target genes.

Collectively, our data support a model where neuronal PPAR δ expression is critical to the function of regulatory neurons involved in energy homeostasis. Profound dysregulation of homeostatic responses to fasting and refeeding, an experimental maneuver to amplify potential defects in the system, reveal UCP2 (whose expression is not de-repressed [53,54]) as a potential molecular mediator of the phenotype. The inability to upregulate UCP2 in response to normal physiological stressors and after feeding raises the possibility that hypothalamic oxidative stress is a key step in obesity pathogenesis, which may be independent of lipotoxicity, at least in this model. Future studies will be required to understand the potential roles of UCP2, inflammation and compensatory changes in other PPAR isoforms in this complex phenotype. Such

studies are warranted, because PPARs are targets of dietary lipids (or metabolites thereof), and are likely to shed important new light upon plausible mechanisms by which a changing dietary environment may multifactorially enhance susceptibility to obesity.

Materials and Methods

Animal care

Mice were housed in a temperature (22°C) and light (12 hour light/dark cycle) controlled room with free access to food and water except where indicated. All studies were approved by the Vanderbilt University Institutional Animal Care and Use Committee and were conducted in accordance with the Guide for the Care and Use of Laboratory Animals.

Neuronal PPAR δ deletion

Neuronal PPAR δ knockout (KO) mice were generated by mating B6.129S4-Ppardtm1Rev/J mice (The Jackson Laboratory) with loxP sites flanking exon 4 of the PPAR δ gene [38] with B6.Cg-Tg(Nes-cre)1Kln/J mice (The Jackson Laboratory) that express Cre recombinase under the control of the rat nestin promoter [67]. Both parental mouse lines were backcrossed to C57BL/6 mice for at least 8 generations prior to breeding. Genotyping for floxed PPAR δ gene exon 4 and Nes-Cre alleles were performed as described [68].

Feeding studies in mice

Mice were fed either a standard laboratory chow diet (LabDiet 5001) or purified, micronutrient matched diets with LF content (Research Diets, D01060501, kcal% = 10% fat, 20% protein, 70% carbohydrate) or HF content (Research Diets, D12451; Kcal% = 45% fat (36% saturated fat), 20% protein, 35% carbohydrate). Body composition was measured by NMR spectroscopy (Bruker Optics).

Energy expenditure

Energy expenditure was assessed by indirect calorimetry in 12 week old chow fed mice and after 20 weeks on HFD. Mice were housed individually in Oxymax cages (Columbus Instruments; Columbus, Ohio). VO $_2$ and VCO $_2$ (mL/hour) were calculated based on the input and output rates of O $_2$ consumption and CO $_2$ production, which were used to determine the respiratory exchange ratio (RER = VCO $_2$ /VO $_2$) and heat (kcal/hour = (3.815 + 1.232 \times RER) \times (VO $_2$)) using the provided software. EE data (kcal/hour) was also normalized to body weight (g) and lean mass (g) measured by NMR the day mice were placed in the chambers.

Histology

Mice were anesthetized with sodium pentobarbital (60 mg/kg) and transcardially perfused with 4% paraformaldehyde. Brains were removed and post-fixed overnight, sucrose embedded, coronally sectioned at 40 μ m and Nissl stained as previously described [69]. Epididymal white adipose tissue samples were fixed for 24 hours in 4% paraformaldehyde, transferred to 70% ethanol before paraffin embedding and staining with hematoxylin and eosin (H&E) stain. Series of nonadjacent sections were processed for each staining protocol. Images were collected at 10 \times magnification using bright field microscopy and qualitatively examined by an experimenter blinded to genotype.

Medial basal hypothalamus wedge dissection

Medial basal hypothalamus dissection was performed as described [70]. Wedges were bisected along the third ventricle in some cases to allow for protein and gene expression analysis.

Leptin sensitivity

Individually housed, male, KO and control (f/f) mice were acclimated to intraperitoneal (i.p.) saline injections (300 μ l) for 7 days. Mice were given an i.p. injection of leptin (5 μ g/g body weight; ProSpec, East Brunswick, NJ) or vehicle (saline) at the onset of the dark period and food intake was measured over 24 hours to assess behavioral leptin sensitivity. Leptin signaling was assessed in a second group of mice treated similarly. Hypothalami were collected 30 minutes after leptin was injected and processed for immunological detection of STAT3 phosphorylation (Tyrosine 705) by Western blot analysis.

Glucose tolerance test

Mice were fasted for four hours prior to receiving an i.p. glucose bolus injection (1 g/kg). Glucose was measured in tail blood obtained from a small incision made at the tip of the tail with a sterile razor blade using a Freestyle handheld glucometer from Abbott Labs (Abbott Park, IL). Glucose levels were measured at various time points over 120 minutes and analyzed by area under the glucose curve from 0–120 minutes.

Plasma hormones and metabolites

Trunk blood was collected at the conclusion of the studies, separated by centrifugation and stored at -80°C . Plasma levels of insulin and leptin were measured by radioimmunoassay (Hormone Assay & Analytical Services Core, Vanderbilt DRTC). Plasma triglycerides and free fatty acid levels were measured using kits from Waco Diagnostics (Richmond, VA). Corticosterone levels were measured as previously described [71].

Fasting-refeeding challenge

Individually housed mice were weighed and food was withdrawn for 24 hours. Weight loss was assessed by a change in body weight at the end of the fasting period. Hyperphagia and weight gain were measured after a 24-hour refeeding period, during which time, the mice had free access to chow diet. Hypothalamic neuropeptide mRNA expression was measured in a second group of mice treated similarly.

Western Blot analysis

Following 33 weeks of HFD or LFD feeding, mice were fasted for 4 hours prior to collecting tissue samples that were then stored at -80°C . Samples were processed for Western blot analysis, as previously described [9], and membranes were probed with primary antibodies against I κ B α , phospho-Y705 STAT3, STAT3 and GAPDH (Cell Signaling; Danvers, MA) followed by HRP conjugated secondary antibodies (Promega; Madison, WI). Protein levels were detected using Western Lightning Plus-ECL Enhanced Chemiluminescence Substrate Kit (Perkin Elmer; Waltham, MA) and image intensity was quantified by densitometry using ImageJ (NIH).

References

- Mokdad AH, Ford ES, Bowman BA, Dietz WH, Vinicor F, et al. (2003) Prevalence of obesity, diabetes, and obesity-related health risk factors, 2001. *JAMA* 289: 76–79.
- Ogden CL, Carroll MD, Curtin LR, McDowell MA, Tabak CJ, et al. (2006) Prevalence of overweight and obesity in the United States, 1999–2004. *JAMA* 295: 1549–1555.

RT-PCR

Total RNA was extracted from frozen hypothalami using the RNeasy kit (Ambion; Austin, TX). cDNA was synthesized using the High Capacity cDNA reverse transcription kit (Applied Biosystems; Carlsbad, CA). The resulting cDNA template was used to quantify mRNA expression via quantitative real-time PCR on a Bio-Rad iCycler using iQ SYBR green Supermix reagent (Bio-Rad; Hercules, CA). Real-time primers were designed using Beacon Design software (Palo Alto, CA). Primer sequences are found in Table S1. Gene expression was normalized to endogenous expression of the housekeeping gene RPL13A.

Brain lipid analysis

Brain lipids were quantified as previously described [72] via extraction using the method of Folch [73], followed by thin layer chromatography (TLC) [74] and quantified using gas chromatographic analysis (GC) (Hormone Assay & Analytical Services Core, Vanderbilt DRTC).

Statistical Analysis

Data are reported as mean \pm SEM. Statistical analysis of differences was analyzed by two-way ANOVA followed by post hoc Bonferroni's multiple comparison test using GraphPad Prism version 5.0 for Windows (San Diego, CA). The student's *t* test for non-paired values was performed when two groups were compared with each other. A *p* value < 0.05 was considered statistically significant.

Supporting Information

Figure S1 Glucose tolerance and corticosterone response in neuronal PPAR δ KO mice. (A) Glucose tolerance test (1 g/kg BW dextrose i.p.) in f/f and KO mice on chow or HFD for 20 weeks ($n = 8–10$). Mice were fasted for 4 hours and glucose measured in tail blood at the indicated time points. (B) Area under the glucose curve (AUC) analysis from glucose tolerance testing. (C) Plasma corticosterone levels in individually housed, chow fed, f/f and KO mice. Blood was collected at nadir (8am), peak (5pm) or 30 minutes after mild restraint stress. Values represent the mean \pm SEM. Statistical significance is denoted in B as ^a ($p < 0.05$ f/f vs. KO, same diet), and ^b ($p < 0.05$ LF vs. HF same genotype), one-way ANOVA and Bonferroni post test. (TIF)

Table S1 Real-time RT PCR primer list. (DOCX)

Acknowledgments

We thank Dr. Alyssa Hasty for scientific advice and Heather Hollis, Dr. Fang Yu and Le Zhang for their excellent technical expertise and assistance.

Author Contributions

Conceived and designed the experiments: HK KN RP OM. Performed the experiments: HK MT GL. Analyzed the data: HK MT GL SD GS KN. Contributed reagents/materials/analysis tools: SD GS LM. Wrote the paper: HK KN.

6. Bray GA, Popkin BM (1998) Dietary fat intake does affect obesity! *Am J Clin Nutr* 68: 1157–1173.
7. Woods SC, Seeley RJ, Rushing PA, D'Alessio D, Tso P (2003) A controlled high-fat diet induces an obese syndrome in rats. *J Nutr* 133: 1081–1087.
8. Maron DJ, Fair JM, Haskell WL (1991) Saturated fat intake and insulin resistance in men with coronary artery disease. The Stanford Coronary Risk Intervention Project Investigators and Staff. *Circulation* 84: 2020–2027.
9. Posey KA, Clegg DJ, Printz RL, Byun J, Morton GJ, et al. (2009) Hypothalamic proinflammatory lipid accumulation, inflammation, and insulin resistance in rats fed a high-fat diet. *Am J Physiol Endocrinol Metab* 296: E1003–1012.
10. De Souza CT, Araujo EP, Bordin S, Ashimine R, Zollner RL, et al. (2005) Consumption of a fat-rich diet activates a proinflammatory response and induces insulin resistance in the hypothalamus. *Endocrinology* 146: 4192–4199.
11. Speed N, Saunders C, Davis AR, Owens WA, Matthies HJ, et al. (2011) Impaired Striatal Akt Signaling Disrupts Dopamine Homeostasis and Increases Feeding. *PLoS One* 6: e25169.
12. Thaler JP, Yi CX, Schur EA, Guyenet SJ, Hwang BH, et al. (2012) Obesity is associated with hypothalamic injury in rodents and humans. *J Clin Invest* 122: 153–162.
13. Issemann I, Green S (1990) Activation of a member of the steroid hormone receptor superfamily by peroxisome proliferators. *Nature* 347: 645–650.
14. Dreyer C, Krey G, Keller H, Givél F, Helftenbein G, et al. (1992) Control of the peroxisomal beta-oxidation pathway by a novel family of nuclear hormone receptors. *Cell* 68: 879–887.
15. Lee CH, Olson P, Evans RM (2003) Minireview: lipid metabolism, metabolic diseases, and peroxisome proliferator-activated receptors. *Endocrinology* 144: 2201–2207.
16. Forman BM, Chen J, Evans RM (1997) Hypolipidemic drugs, polyunsaturated fatty acids, and eicosanoids are ligands for peroxisome proliferator-activated receptors alpha and delta. *Proc Natl Acad Sci U S A* 94: 4312–4317.
17. Braissant O, Fufelle F, Scotto C, Dauca M, Wahli W (1996) Differential expression of peroxisome proliferator-activated receptors (PPARs): tissue distribution of PPAR-alpha, -beta, and -gamma in the adult rat. *Endocrinology* 137: 354–366.
18. Chawla A, Schwarz EJ, Dimaculangan DD, Lazar MA (1994) Peroxisome proliferator-activated receptor (PPAR) gamma: adipose-predominant expression and induction early in adipocyte differentiation. *Endocrinology* 135: 798–800.
19. Kersten S, Seydoux J, Peters JM, Gonzalez FJ, Desvergne B, et al. (1999) Peroxisome proliferator-activated receptor alpha mediates the adaptive response to fasting. *J Clin Invest* 103: 1489–1498.
20. Auwerx J, Schoonjans K, Fruchart JC, Staels B (1996) Transcriptional control of triglyceride metabolism: fibrates and fatty acids change the expression of the LPL and apo C-III genes by activating the nuclear receptor PPAR. *Atherosclerosis* 124 Suppl: S29–37.
21. Lee SS, Pineau T, Drago J, Lee EJ, Owens JW, et al. (1995) Targeted disruption of the alpha isoform of the peroxisome proliferator-activated receptor gene in mice results in abolishment of the pleiotropic effects of peroxisome proliferators. *Mol Cell Biol* 15: 3012–3022.
22. Dressel U, Allen TL, Pippal JB, Rohde PR, Lau P, et al. (2003) The peroxisome proliferator-activated receptor beta/delta agonist, GW501516, regulates the expression of genes involved in lipid catabolism and energy uncoupling in skeletal muscle cells. *Mol Endocrinol* 17: 2477–2493.
23. Wang YX, Zhang CL, Yu RT, Cho HK, Nelson MC, et al. (2004) Regulation of muscle fiber type and running endurance by PPARdelta. *PLoS Biol* 2: e294.
24. Peters JM, Lee SST, Li W, Ward JM, Gavrilova O, et al. (2000) Growth, Adipose, Brain, and Skin Alterations Resulting from Targeted Disruption of the Mouse Peroxisome Proliferator-Activated Receptor beta (delta). *Mol Cell Biol* 20: 5119–5128.
25. Miyachi H (2007) Design, synthesis, and structure-activity relationship study of peroxisome proliferator-activated receptor (PPAR) delta-selective ligands. *Curr Med Chem* 14: 2335–2343.
26. Yessoufou A, Wahli W (2010) Multifaceted roles of peroxisome proliferator-activated receptors (PPARs) at the cellular and whole organism levels. *Swiss Med Wkly* 140: w13071.
27. Bright JJ, Kanakasabai S, Chearwae W, Chakraborty S (2008) PPAR Regulation of Inflammatory Signaling in CNS Diseases. *PPAR Res* 2008: 658520.
28. Moreno S, Farioli-Vecchioli S, Ceru MP (2004) Immunolocalization of peroxisome proliferator-activated receptors and retinoid X receptors in the adult rat CNS. *Neuroscience* 123: 131–145.
29. Lu M, Sarruf DA, Talukdar S, Sharma S, Li P, et al. (2011) Brain PPAR-[gamma] promotes obesity and is required for the insulin-sensitizing effect of thiazolidinediones. *Nat Med* 17: 618–622.
30. Ryan KK, Li B, Grayson BE, Matter EK, Woods SC, et al. (2011) A role for central nervous system PPAR-gamma in the regulation of energy balance. *Nat Med* 17: 623–626.
31. Chakravarthy MV, Zhu Y, Lopez M, Yin L, Wozniak DF, et al. (2007) Brain fatty acid synthase activates PPARalpha to maintain energy homeostasis. *J Clin Invest* 117: 2539–2552.
32. Xing G, Zhang L, Heynen T, Yoshikawa T, Smith M, et al. (1995) Rat PPAR delta contains a CGG triplet repeat and is prominently expressed in the thalamic nuclei. *Biochem Biophys Res Commun* 217: 1015–1025.
33. Woods JW, Tanen M, Figueroa DJ, Biswas C, Zychband E, et al. (2003) Localization of PPARdelta in murine central nervous system: expression in oligodendrocytes and neurons. *Brain Res* 975: 10–21.
34. Kalinin S, Richardson JC, Feinstein DL (2009) A PPARdelta agonist reduces amyloid burden and brain inflammation in a transgenic mouse model of Alzheimer's disease. *Curr Alzheimer Res* 6: 431–437.
35. Dunn SE, Bhat R, Straus DS, Sobel RA, Axtell R, et al. (2010) Peroxisome proliferator-activated receptor delta limits the expansion of pathogenic Th cells during central nervous system autoimmunity. *J Exp Med* 207: 1599–1608.
36. Schnegg CI, Robbins ME (2011) Neuroprotective Mechanisms of PPARdelta: Modulation of Oxidative Stress and Inflammatory Processes. *PPAR Res* 2011: 373560.
37. Sauer B, Henderson N (1989) Cre-stimulated recombination at loxP-containing DNA sequences placed into the mammalian genome. *Nucleic Acids Res* 17: 147–161.
38. Barak Y, Liao D, He W, Ong ES, Nelson MC, et al. (2002) Effects of peroxisome proliferator-activated receptor delta on placenta, adiposity, and colorectal cancer. *Proc Natl Acad Sci U S A* 99: 303–308.
39. Dubois NC, Hofmann D, Kaloulis K, Bishop JM, Trumpp A (2006) Nestin-Cre transgenic mouse line Nes-Cre1 mediates highly efficient Cre/loxP mediated recombination in the nervous system, kidney, and somite-derived tissues. *Genesis* 44: 355–360.
40. Friedman JM (2002) The function of leptin in nutrition, weight, and physiology. *Nutr Rev* 60: S1–14; discussion S68–84, 85–17.
41. Levin BE, Dunn-Meynell AA (2002) Reduced central leptin sensitivity in rats with diet-induced obesity. *Am J Physiol Regul Integr Comp Physiol* 283: R941–948.
42. Vaisse C, Halaas JL, Horvath CM, Darnell JE Jr, Stoffel M, et al. (1996) Leptin activation of Stat3 in the hypothalamus of wild-type and ob/ob mice but not db/db mice. *Nat Genet* 14: 95–97.
43. Georgiadi A, Lichtenstein L, Degenhardt T, Boekschoten MV, van Bilsen M, et al. (2010) Induction of cardiac Angptl4 by dietary fatty acids is mediated by peroxisome proliferator-activated receptor beta/delta and protects against fatty acid-induced oxidative stress. *Circ Res* 106: 1712–1721.
44. Alvarez-Guardia D, Palomer X, Coll T, Serrano L, Rodriguez-Calvo R, et al. (2011) PPARbeta/delta activation blocks lipid-induced inflammatory pathways in mouse heart and human cardiac cells. *Biochim Biophys Acta* 1811: 59–67.
45. Karin M, Ben-Neriah Y (2000) Phosphorylation meets ubiquitination: the control of NF-[kappa]B activity. *Annu Rev Immunol* 18: 621–663.
46. Schwartz MW, Erickson JC, Baskin JC, Palmiter RD (1998) Effect of fasting and leptin deficiency on hypothalamic neuropeptide Y gene transcription in vivo revealed by expression of a lacZ reporter gene. *Endocrinology* 139: 2629–2635.
47. Andrews ZB, Liu ZW, Wallingford N, Erion DM, Borok E, et al. (2008) UCP2 mediates ghrelin's action on NPY/AgRP neurons by lowering free radicals. *Nature* 454: 846–851.
48. Weinberg JM (2006) Lipotoxicity. *Kidney Int* 70: 1560–1566.
49. Coll T, Alvarez-Guardia D, Barroso E, Gomez-Foix AM, Palomer X, et al. (2010) Activation of peroxisome proliferator-activated receptor-{delta} by GW501516 prevents fatty acid-induced nuclear factor-{kappa}B activation and insulin resistance in skeletal muscle cells. *Endocrinology* 151: 1560–1569.
50. Wu HT, Chen CT, Cheng KC, Li YX, Yeh CH, et al. (2011) Pharmacological activation of peroxisome proliferator-activated receptor delta improves insulin resistance and hepatic steatosis in high fat diet-induced diabetic mice. *Horm Metab Res* 43: 631–635.
51. Frederich RC, Lollmann B, Hamann A, Napolitano-Rosen A, Kahn BB, et al. (1995) Expression of ob mRNA and its encoded protein in rodents. Impact of nutrition and obesity. *J Clin Invest* 96: 1658–1663.
52. Sutton GM, Trevaskis JL, Hulver MW, McMillan RP, Markward NJ, et al. (2006) Diet-genotype interactions in the development of the obese, insulin-resistant phenotype of C57BL/6J mice lacking melanocortin-3 or -4 receptors. *Endocrinology* 147: 2183–2196.
53. Shi Y, Hon M, Evans RM (2002) The peroxisome proliferator-activated receptor delta, an integrator of transcriptional repression and nuclear receptor signaling. *Proc Natl Acad Sci U S A* 99: 2613–2618.
54. Adhikary T, Kaddatz K, Finkernagel F, Schonbauer A, Meissner W, et al. (2011) Genomewide analyses define different modes of transcriptional regulation by peroxisome proliferator-activated receptor-beta/delta (PPARbeta/delta). *PLoS One* 6: e16344.
55. Lee CH, Kang K, Mehl IR, Nofsinger R, Alaynick WA, et al. (2006) Peroxisome proliferator-activated receptor delta promotes very low-density lipoprotein-derived fatty acid catabolism in the macrophage. *Proc Natl Acad Sci U S A* 103: 2434–2439.
56. Li Y, Cheng L, Qin Q, Liu J, Lo WK, et al. (2009) High-fat feeding in cardiomyocyte-restricted PPARdelta knockout mice leads to cardiac overexpression of lipid metabolic genes but fails to rescue cardiac phenotypes. *J Mol Cell Cardiol* 47: 536–543.
57. Lee CH, Chawla A, Urbiztondo N, Liao D, Boisvert WA, et al. (2003) Transcriptional repression of atherogenic inflammation: modulation by PPARdelta. *Science* 302: 453–457.
58. Arsenijevic D, de Bilbao F, Plamondon J, Paradis E, Vallet P, et al. (2006) Increased infarct size and lack of hyperphagic response after focal cerebral ischemia in peroxisome proliferator-activated receptor beta-deficient mice. *J Cereb Blood Flow Metab* 26: 433–445.
59. Diano S, Liu ZW, Jeong JK, Dietrich MO, Ruan HB, et al. (2011) Peroxisome proliferation-associated control of reactive oxygen species sets melanocortin tone and feeding in diet-induced obesity. *Nat Med*.

60. Horvath TL, Diano S, Miyamoto S, Barry S, Gatti S, et al. (2003) Uncoupling proteins-2 and 3 influence obesity and inflammation in transgenic mice. *Int J Obes Relat Metab Disord* 27: 433–442.
61. Bai Y, Onuma H, Bai X, Medvedev AV, Misukonis M, et al. (2005) Persistent nuclear factor-kappa B activation in Ucp2 $^{-/-}$ mice leads to enhanced nitric oxide and inflammatory cytokine production. *J Biol Chem* 280: 19062–19069.
62. Haines BA, Mehta SL, Pratt SM, Warden CH, Li PA (2010) Deletion of mitochondrial uncoupling protein-2 increases ischemic brain damage after transient focal ischemia by altering gene expression patterns and enhancing inflammatory cytokines. *J Cereb Blood Flow Metab* 30: 1825–1833.
63. Degasperi GR, Romanatto T, Denis RG, Araujo EP, Moraes JC, et al. (2008) UCP2 protects hypothalamic cells from TNF-alpha-induced damage. *FEBS Lett* 582: 3103–3110.
64. Konig B, Rauer C, Rosenbaum S, Brandsch C, Eder K, et al. (2009) Fasting Upregulates PPARalpha Target Genes in Brain and Influences Pituitary Hormone Expression in a PPARalpha Dependent Manner. *PPAR Res* 2009: 801609.
65. Gustafsson MC, Knight D, Palmer CN (2009) Ligand modulated antagonism of PPARgamma by genomic and non-genomic actions of PPARdelta. *PLoS One* 4: e7046.
66. Bugge A, Mandrup S (2010) Molecular Mechanisms and Genome-Wide Aspects of PPAR Subtype Specific Transactivation. *PPAR Res* 2010.
67. Tronche F, Kellendonk C, Kretz O, Gass P, Anlag K, et al. (1999) Disruption of the glucocorticoid receptor gene in the nervous system results in reduced anxiety. *Nat Genet* 23: 99–103.
68. Truett GE, Heeger P, Mynatt RL, Truett AA, Walker JA, et al. (2000) Preparation of PCR-quality mouse genomic DNA with hot sodium hydroxide and tris (HotSHOT). *Biotechniques* 29: 52, 54.
69. Stanwood GD, Leitch DB, Savchenko V, Wu J, Fitsanakis VA, et al. (2009) Manganese exposure is cytotoxic and alters dopaminergic and GABAergic neurons within the basal ganglia. *J Neurochem* 110: 378–389.
70. Sasaki T, Kim HJ, Kobayashi M, Kitamura YI, Yokota-Hashimoto H, et al. (2010) Induction of hypothalamic Sirt1 leads to cessation of feeding via agouti-related peptide. *Endocrinology* 151: 2556–2566.
71. Boyle MP, Brewer JA, Funatsu M, Wozniak DF, Tsien JZ, et al. (2005) Acquired deficit of forebrain glucocorticoid receptor produces depression-like changes in adrenal axis regulation and behavior. *Proc Natl Acad Sci U S A* 102: 473–478.
72. Saraswathi V, Hasty AH (2006) The role of lipolysis in mediating the proinflammatory effects of very low density lipoproteins in mouse peritoneal macrophages. *J Lipid Res* 47: 1406–1415.
73. Folch J, Lees M, Sloane Stanley GH (1957) A simple method for the isolation and purification of total lipides from animal tissues. *J Biol Chem* 226: 497–509.
74. Morrison WR, Smith LM (1964) Preparation of Fatty Acid Methyl Esters and Dimethylacetals from Lipids with Boron Fluoride–Methanol. *J Lipid Res* 5: 600–608.